ACI MATERIALS JOURNAL TECHNICAL PAPER

Title No. 121-M25

# Multi-Approaches to Improve Internally Cured Concrete for Rigid Pavement Application

by Sangyoung Han, Thanachart Subgranon, Hung-Wen Chung, Kukjoo Kim, and Mang Tia

*A comprehensive laboratory testing program, field-testing program, numerical analysis, and life-cycle cost analysis were conducted to evaluate the beneficial effects of incorporating shrinkage-reducing admixture (SRA), polymeric microfibers (PMFs), and optimized aggregate gradation (OAG) into internally cured concrete (ICC) mixtures for rigid pavement applications. Results from the laboratory program indicate that all the ICC mixtures outperformed the standard concrete (SC) mixture. All the ICC mixtures showed a decrease in drying shrinkage compared to the SC mixture. Based on the laboratory program, three ICC mixtures and one SC mixture were selected for the full-scale test and subjected to a heavy vehicle simulator for accelerated fatigue testing. Extensive testing and analysis have shown that ICC mixtures incorporating SRA, PMFs, and OAG can be beneficially used in pavement applications to achieve increased pavement life.*

**Keywords:** critical stress analysis; full-scale test slabs; internally cured concrete (ICC); optimized aggregate gradation (OAG); polymeric microfibers (PMFs); shrinkage-reducing admixture (SRA).

## INTRODUCTION

High-strength concrete (HSC) and high-performance concrete (HPC) mixtures have gained popularity in recent years because of their potential long-term benefits in performance.[1] However, these types of concrete generally exhibit a substantial magnitude of autogenous shrinkage due to the lower water-cement ratio (*w*/*c*) and finer pore constitutions.[2,3] Additionally, for these modern concrete mixtures, the blended cement matrix incorporating fly ash, slag, and silica fume has been preferred over pure portland cement owing to their various benefits, such as improved integrity, enhanced sustainability, and reduced cost. Nevertheless, blended cementitious materials require additional curing water because the shrinkage accompanying the pozzolanic and hydraulic reactions of these cement replacements is substantial when compared with that of pure portland cement.[4,5] Given the characteristics of modern concrete mixtures, using modern concrete with insufficient hydrating water increases the potential risk of shrinkage cracking at an early age, which can cause structural deficiencies and instability.

In coping with the shrinkage cracking of modern concrete at early ages, the internal curing (IC) technique has been successfully introduced by the concept that water can be embedded in the concrete through water-filled components such as expanded lightweight aggregate (LWA), superabsorbent polymers, and cellulose fibers.[6,7] In particular, the use of saturated LWA as water-filled inclusion has been widely used in North America. LWA is a highly porous material that can be used as a replacement for natural coarse and/or fine aggregate.[8] When saturated, each LWA particle acts like a small reservoir inside the concrete, which will release water to the surrounding cement paste during its hydration stage. This mechanism helps to prevent the self-desiccation phenomenon and promote the hydration of the cement, thereby alleviating the degree of autogenous cracking.[9-12] Additionally, using LWA offers other improved properties, including increased workability,[13] higher ultimate strength,[14] reduced likelihood of thermal cracking,[15] improved freezing-and-thawing resistance,[16] and improved transport properties, such as reduced permeability, ion diffusion, and sorption.[14]

In addition to the aforementioned benefits in the aspects of plastic, hardened, and durable properties, using internally cured concrete (ICC) in the rigid pavement structure significantly helps reduce the moisture-related curling/wrapping magnitude and drying shrinkage, which decrease pavement serviceability.[17,18] High levels of curling deformations in pavements have been correlated to issues of rideability,[19] cracking,[20] and durability.[21] As a result, numerous studies have documented the widespread use of ICC in various types of pavements for mitigating the issues of curling/wrapping and drying shrinkage.[22]

The majority of the literature has focused on the beneficial effects of ICC on pavement structure, particularly in reducing curling magnitudes and drying shrinkage. However, these studies have been limited to identifying the effect of only one method of IC inclusion in the concrete mixture. In contrast, the current study considered both IC inclusion and design-enhanced techniques that are expected to maximize the benefits of the ICC mixture (referred to as the hybrid ICC mixture hereafter). The ICC mixtures were evaluated by incorporating the enhanced techniques, including a shrinkage-reducing admixture (SRA), polymeric microfibers (PMFs), and optimized aggregate gradation (OAG), and were compared to a concrete mixture without ICC. In this study, a laboratory testing program, a full-scale field-testing program, and a numerical analysis were performed to investigate and maximize the benefits of the hybrid ICC mixture in rigid pavement applications.

To identify the suitable concrete mixture for rigid pavement applications, a comprehensive testing program was carried out. This program included both laboratory and full-scale field-testing programs to evaluate the combined

*ACI Materials Journal*, V. 121, No. 3, May 2024.
MS No. M-2023-055.R1, doi: 10.14359/51740564, received October 18, 2023, and reviewed under Institute publication policies. 

effects of incorporating SRA, PMFs, and OAG techniques in standard concrete (SC) and ICC. Based on the laboratory test results and evaluation, three ICC mixtures and one SC mixture were selected to be evaluated in full-size pavement test slabs, which were subjected to loading by a heavy vehicle simulator (HVS). Finally, finite element (FE) analysis was employed to assess the structural performance of these concrete mixtures for pavement applications.

## EFFECT OF ENHANCED TECHNIQUES

### Effect of shrinkage-reducing admixture on pavement applications

Numerous researchers have emphasized using SRAs in pavement structures to mitigate the risks of early-age and long-term shrinkage cracking.[23-25] When incorporated into concrete, SRAs have been shown to attenuate shrinkage resulting from drying or self-desiccation.[26,27] Consequently, for scenarios where pavement curling and drying shrinkage are anticipated challenges, incorporating SRAs into the concrete mixture is strongly advocated to alleviate these concerns. This study evaluated the characteristics of the ICC mixture with and without SRAs to better understand the combined effects of using LWA and SRA in concrete pavement.

### Effect of fiber-reinforced concrete on pavement applications

According to the literature, the use of fiber-reinforced concrete (FRC) has been shown to have several benefits over SC. FRC has a higher ultimate strength and toughness, as well as reduced shrinkage cracking, improved permeability resistance, and delayed macrocracking.[28-30] These advantages come from the fibers' anchoring of the concrete materials, which favors cohesiveness, tensile strength, and permeability. Although FRC has some limitations in structural applications because the fibers are randomly positioned and not aligned with the main stress directions, its efficacy in pavement applications is notable, especially in its capacity to modulate crack width and postpone initial cracking.[31] Depending on the dosages of incorporated macro-synthetic fibers, one can adhere to these general guidelines: a low dosage ranging from 1.8 to 2.4 kg/m$^3$ (0.11 to 0.15 lb/ft$^3$) can augment crack control and toughness; a medium dosage of 2.4 to 4.2 kg/m$^3$ (0.15 to 0.26 lb/ft$^3$) can extend the spacing between the control joints; and a high dosage starting at 4.5 kg/m$^3$ (0.28 lb/ft$^3$) can significantly expand joint spacing, even prompting consideration for joint-free pavements akin to continuously reinforced concrete pavement (CRCP).[32,33]

In this study, the choice of fibers was carefully considered, and microfibers (diameter less than 0.022 mm [0.000867 in.]) were selected over macrofibers (0.5 mm [0.02 in.] diameter). Microfibers were proven not only to significantly improve ultimate strength and toughness far beyond that of macrofibers but also to have less impact on the workability of the fresh concrete.[28,34] The synthetic fiber used in this study was also attractive due to its good chemical stability, low density, and efficient mixing characteristics compared to metallic fibers.[35] As a result, a PMF was chosen for use in this study to evaluate ICC performance with or without PMFs.

### Effect of optimized aggregate gradation on pavement applications

It is widely recognized that the nominal size, gradation, and proportions of aggregates are important factors affecting the plastic and hardened properties of the concrete.[36] The concept of the OAG is to constitute well-distributed aggregates by controlling the proportion of the different-sized aggregates, typically at least three different categorized aggregates.[37] The application of OAG in the concrete mixture design can enable the cement matrix to fill in the space between aggregates more homogeneously, which in turn can directly enhance both hydration and strength development. With this favorable phenomenon from designing concrete based on the OAG technique, a targeted compressive strength[38] and better workability[39] were effectively gained from OAG concrete even though less cementitious material was used than in SC. To identify the potential effects of the OAG technique on the ICC mixture as pavement application, the two following cement-paste contents were used: 100% and 90% of the paste quantity of the SC mixture.

This paper employed the modified OAG proposed by Lindquist et al.[37] This method was used to proportion the virgin coarse aggregate, virgin fine aggregate, and LWA components forming the concrete mixtures under evaluation. One of the key tools for assessing the mixture's properties is the coarseness factor chart, which plots the coarseness factor (CF) against the workability factor (WF).

$$\mathrm{CF} = Q \div (Q + I) \times 100 \quad (1)$$

where $Q$ is the percent retained on 37.5 + 25.0 + 19.0 + 12.5 + 9.5 mm (1.48 + 0.98 + 0.75 + 0.49 + 0.37 in.); and $I$ is the percent retained on 4.75 + 2.36 mm (0.19 + 0.09 in.). The WF of a concrete mixture can be calculated as follows

$$\mathrm{WF} = W \div (Q + I + W) \times 100 + CCF \quad (2)$$

where $W$ is the percent retained on 1.18 + 0.6 + 0.3 + 0.15 + 0.075 mm (0.05 + 0.02 + 0.01 + 0.006 + 0.003 in.) + pan (sieve); and $CCF = 2.5 \times (C - 335) + 56$ (where $C$ is the amount of cement in kg/m$^3$).

To determine the workability of a specific concrete mixture, both the CF and WF are plotted on this chart. Ideally, a concrete mixture with an OAG should fall within the workability box. This box's boundaries are delineated by the corner coordinates, as advised by the Montana Department of Transportation (MDT).[40] A mixture that plots within this box is considered favorable and will likely result in a workable concrete mixture that can be placed and finished easily and will have good long-term performance.

By adhering to the OAG procedure outlined by Lindquist et al.,[37] this study ascertained optimized proportions of coarse and fine aggregates in the different concrete mixtures containing LWA. Furthermore, MDT[40] designates the ideal target line in the percent retained chart (notably, the haystack gradation, a humped curve line based on an "8-18" band gradation of percent retained aggregate on each sieve).

## RESEARCH SIGNIFICANCE

Although extensive research has been carried out on the effect of ICC on rigid pavements for enhancing serviceability and durability, no study has been done to evaluate the effects of other enhancing techniques on ICC. This study investigated the effects of using PMFs, OAG, and SRA on ICC by means of a laboratory testing program, full-scale pavement tests, and numerical analysis. The results from this study can be used to optimize the use of these enhanced techniques on ICC for rigid pavement applications.

## EVALUATION OF CONCRETE MIXTURES IN LABORATORY PROGRAM

### Concrete mixture design

The ICC mixtures were compared to the SC mixture for the construction of concrete pavement slabs with a *w*/*c* of 0.44. To investigate the ICC in terms of mechanical performance, the following different enhanced techniques were incorporated: PMF, OAG, and SRA. The designed volumetric proportions of these mixtures are shown in Fig. 1, and the detailed numerical mixture design is presented in Table 1. Table 2 presents the properties of the natural different-sized aggregates and LWA used. All used aggregates were

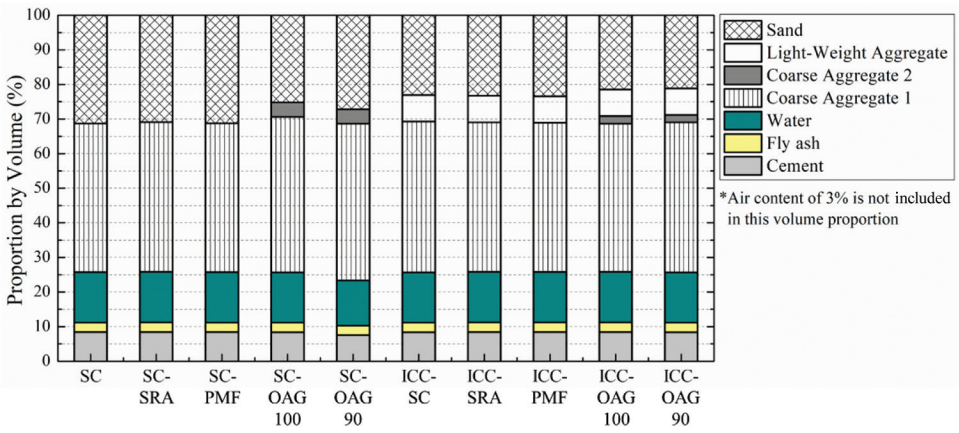


*Fig. 1—Proportions of concrete mixture design by volume.*

**Table 1—Concrete mixture design for laboratory testing program**

| Selected concrete mixtures | SC (control) | SC-SRA | SC-PMF | SC-OAG 100 | SC-OAG 90 | ICC (control) | ICC-SRA | ICC-PMF | ICC-OAG 100 | ICC-OAG 90 |
|---|---|---|---|---|---|---|---|---|---|---|
| Cement, kg/m$^3$ | 256.3 | 256.3 | 256.3 | 256.3 | 230.8 | 256.3 | 256.3 | 256.3 | 256.3 | 230.8 |
| Fly ash, kg/m$^3$ | 64.1 | 64.1 | 64.1 | 64.1 | 57.5 | 64.1 | 64.1 | 64.1 | 64.1 | 57.5 |
| Water, kg/m$^3$ | 141.2 | 141.2 | 141.2 | 141.2 | 127.0 | 141.2 | 141.2 | 141.2 | 141.2 | 127.0 |
| Coarse aggregate 1, kg/m$^3$ | 873.9 | 998.5 | 1003.2 | 1009.2 | 1020.4 | 1006.2 | 1002.0 | 1003.8 | 967.0 | 960.5 |
| Coarse aggregate 2, kg/m$^3$ | — | — | — | 151.9 | 150.7 | — | — | — | 86.6 | 128.1 |
| Lightweight aggregate, kg/m$^3$ | — | — | — | — | — | 113.9 | 113.9 | 113.9 | 113.9 | 106.2 |
| Fine aggregate, kg/m$^3$ | 812.8 | 803.3 | 811.0 | 640.1 | 691.8 | 604.5 | 606.3 | 612.9 | 552.9 | 602.8 |
| Air entrainer, mL/kg | 0.02 | 0.09 | 0.09 | 0.06 | 0.08 | 0.00 | 0.12 | 0.15 | 0.12 | 0.08 |
| Water reducer, mL/kg | 3.0 | 3.0 | 3.1 | 2.9 | 2.9 | 2.9 | 2.9 | 2.9 | 2.9 | 3.1 |
| High-range water reducer, mL/kg | 3.5 | 3.6 | 3.1 | 1.1 | 2.7 | 2.2 | 1.9 | 2.2 | 1.9 | 3.7 |
| Shrinkage-reducing admixture, mL/kg | — | 12.8 | — | — | — | — | 12.8 | — | — | — |
| Synthetic microfiber, kg/m$^3$ | — | — | 0.9 | — | — | — | — | 0.9 | — | — |

Note: 1 kg/m$^3$ = 0.062 lb/ft$^3$; 1 mL/kg = 0.015 fl. oz./lb.

**Table 2—Specific gravity and water absorption of aggregates used**

| Four aggregates used | Coarse aggregate 1 | Coarse aggregate 2 | Fine aggregate | Lightweight aggregate |
|---|---|---|---|---|
| Bulk specific gravity (saturated surface-dry) | 2.428 | 2.452 | 2.651 | 1.538 |
| Bulk specific gravity (dry) | 2.343 | 2.354 | 2.633 | 1.229 |
| Apparent specific gravity (dry) | 2.559 | 2.608 | 2.640 | 1.802 |
| Water absorption, % | 3.6 | 4.2 | 0.3 | 25.8 |
| Aggregate type | Limestone | Limestone | Sand | Expanded clay |
| Aggregate source | Florida | Florida | Florida | Louisiana |

tested for their physical and chemical properties and satisfied the requirements of ASTM C1761/C1761M.

Moreover, for the mixtures incorporating the OAG technique, the following cement-paste contents were used: 100% and 90% of the paste quantity of the SC mixture. To improve the optimized gradation, two different natural coarse aggregates were used. Coarse aggregate 1 had a nominal maximum size of 25.4 mm (1 in.), and coarse aggregate 2 had a nominal maximum size of 9.5 mm (0.37 in.). For the ICC mixtures, a part of the fine aggregate was replaced with the pre-wetted LWAs of expanded clay. The quantity of LWA used was an amount that supplied 3.2 kg (7 lb) of absorbed water per 45.4 kg (100 lb) of cement used. Figure 2 shows the gradation chart of the selected aggregates in this study. All batching, mixing, casting, and curing processes were performed in the conventional method.

## Concrete mixture properties

From 10 concrete mixtures evaluated in the laboratory testing program, one SC and three ICC mixtures with the best potential performance were selected to be used in two separate full-scale test slabs. Two main attributes considered in making the selection were the workability of the fresh concrete and the properties of the hardened concrete. Table 3 presents the plastic properties of the 10 concrete mixtures compared to Florida Department of Transportation (FDOT) specifications from the laboratory testing program.[41] For the plastic properties, the slump, air content, temperature, and unit weight data were measured in accordance with ASTM standards: ASTM C143/C143M, ASTM C231/C231M, ASTM C1064/C1064M, and ASTM C138/C138M. In summary, all mixtures showed good performance in terms of plastic properties. All mixtures were judged as suitable for the rigid pavement applications based on FDOT specifications.

Three categories of properties of hardened concrete are critical to assessing the performance of rigid pavement applications in terms of strength, drying shrinkage, and permeability, indicated by rapid chloride penetration (RCP). For the strength properties, the compressive strength, modulus of rupture (MOR), and modulus of elasticity (MOE) data are shown in Fig. 3. All concrete mixtures have suitable strengths for pavement applications that meet the allowable requirement according to the AASHTO specification.[42] Note that all hardened properties were determined with an average value of three samples for each test.

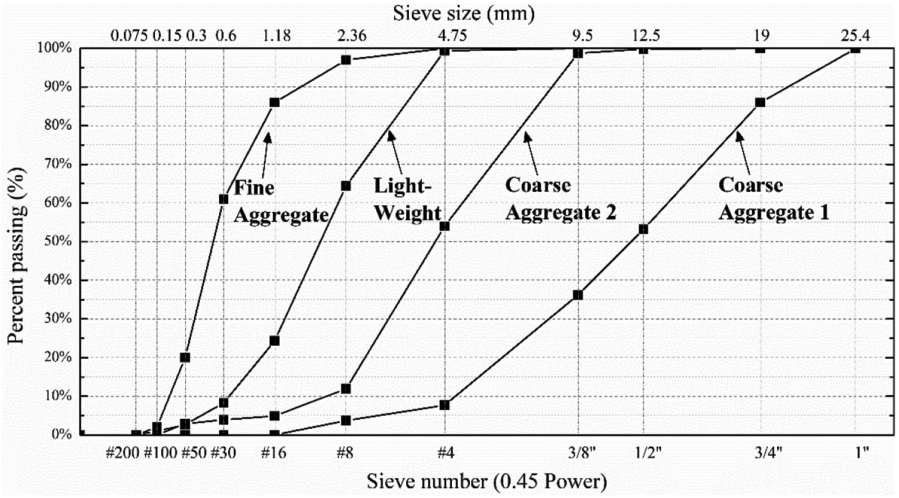


*Fig. 2—Gradation of aggregates used in study.*

**Table 3—Concrete plastic properties**

| Concrete mixtures | Slump, cm | Air content, % | Temperature, °C | Unit weight, kg/m$^3$ |
|---|---|---|---|---|
| SC (control) | 12.7 | 4.7 | 22.8 | 2249 |
| SC-SRA | 6.35 | 3.3 | 23.9 | 2268 |
| SC-PMF | 11.4 | 4.6 | 23.3 | 2225 |
| SC-OAG 100 | 4.5 | 2.1 | 23.9 | 2313 |
| SC-OAG 90 | 7.6 | 3.6 | 24.7 | 2292 |
| ICC (control) | 5.7 | 2.7 | 24.1 | 2227 |
| ICC-SRA | 7.0 | 3.9 | 21.9 | 2204 |
| ICC-PMF | 3.0 | 2.6 | 23.3 | 2243 |
| ICC-OAG 100 | 6.4 | 2.2 | 23.9 | 2249 |
| ICC-OAG 90 | 7.6 | 3.5 | 23.9 | 2196 |
| FDOT specification | 2.5 to 12.7 | 1 to 6 | 20 to 30 | — |

Note: 1 cm = 0.39 in.; °F = (°C × 9/5) + 32; 1 kg/m$^3$ = 0.062 lb/ft$^3$.

More importantly, one of the key factors to evaluate structural performance is the ratio of the MOR over the MOE (*R*/*E*). For several published studies, MOR has been used as the independent indicator to evaluate the resistance of fatigue cracking; the risk of fatigue cracking decreases as MOR increases.[43] Meanwhile, a lower MOE yields lower residual stresses, closely correlated to the reduction of the potential cracking when the same loading is applied.[14,44] In general, the MOE of the concrete increases as the concrete strength, such as compressive strength and MOR, increases. A higher-strength concrete mixture is recommended, but higher stress is simultaneously involved in the concrete structure due to increased MOE. Therefore, the desirable concrete mixture has an appropriate combination of MOR and MOE, which can be expressed by a high ratio of *R*/*E*. In this study, *R*/*E* was used to evaluate the potential structural performance of the concrete mixtures from the laboratory program. Figure 3 also exhibits the *R*/*E* of all the mixtures. The ICC concrete mixtures show improvement in the *R*/*E*, especially the three mixtures of ICC-PMF, ICC-ACO 100, and ICC-ACO 90, which substantially increased the *R*/*E* compared to the non-ICC concrete mixtures.

Table 4 shows the results from the laboratory program of the coefficient of thermal expansion (CTE), drying

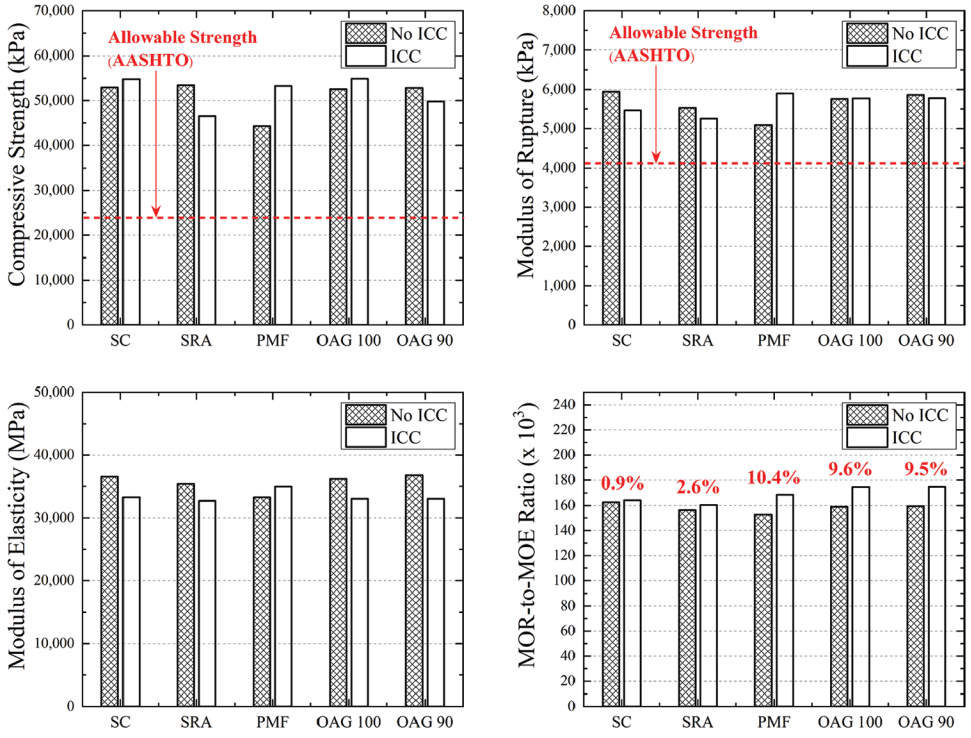


*Fig. 3—Hardened concrete properties at 28 days from laboratory testing program: (top left) compressive strength of each concrete mixture; (top right) MOR of each concrete mixture; (bottom left) MOE of each concrete mixture; and (bottom right) key factor of* R/E *for evaluation of each concrete mixture.*

**Table 4—Concrete CTE, shrinkage, and permeability properties at 28 days**

| Concrete mixtures | CTE, με/°F | | Surface resistivity, kΩ·cm | | Rapid chloride permeability, coulombs | |
|---|---|---|---|---|---|---|
| | 28 days | 365 days | 28 days | 365 days | 28 days | 365 days |
| SC (control) | 4.41 | 5.20 | 10.0 | 45.4 | 3579 | 710 |
| SC-SRA | 4.57 | 5.32 | 10.0 | 41.2 | 4166 | 729 |
| SC-PMF | 3.66 | 5.23 | 9.9 | 38.1 | 4131 | 771 |
| SC-OAG 100 | 4.42 | 4.48 | 9.6 | 46.3 | 3820 | 758 |
| SC-OAG 90 | 4.70 | 4.54 | 10.1 | 44.8 | 3769 | 768 |
| ICC (control) | 3.79 | 4.97 | 10.5 | 45.5 | 3902 | 662 |
| ICC-SRA | 4.21 | 5.22 | 11.1 | 49.1 | 3413 | 614 |
| ICC-PMF | 3.66 | 4.18 | 11.8 | 50.4 | 3354 | 586 |
| ICC-OAG 100 | 3.56 | 4.19 | 11.1 | 49.7 | 3755 | 650 |
| ICC-OAG 90 | 4.44 | 4.28 | 12.4 | 48.2 | 3339 | 542 |
| AASHTO specification | — | | Moderate: 10<br>Low: 20 | | Low: 2000<br>Very low: 20,000 | |

shrinkage, and permeability for the concrete mixtures at 28 days. The tests of CTE, drying shrinkage, surface resistivity, and RCP were conducted in accordance with standards such as AASHTO T 336, ASTM C157, FM 5-579, and ASTM C1202. Studies on the performance of concrete pavement recommended using lower CTE and shrinkage to reduce the thermal and built-in stresses.[45] Additionally, a reduced concrete permeability will prevent the penetration of water, gas, and ions into the hardened concrete, which may result in structure deficiencies pertaining to freezing and thawing, sulfate attack, and alkali-aggregate reaction.[46] All the concrete mixtures had a minimal length change both in contraction and expansion as well as acceptable permeability according to AASHTO specifications.[42]

One of the primary goals of using IC in the concrete mixture was to alleviate the possibility of cracking, which can be indirectly evaluated with the degree of drying shrinkage. To evaluate long-term performance, the length changes due to the effect of drying shrinkage were measured for 2 years in this laboratory program. Figure 4 shows the time-series drying shrinkage for the ICC mixtures compared to the control mixture of SC. It is noted that the hybrid ICC mixtures with SRA, PMFs, and OAG had considerably lower drying shrinkage than the SC mixture. This reduction can be largely attributed to the provision of IC water by the ICC, which inherently mitigates drying shrinkage.

## Concrete mixture selection

The concrete mixtures from the laboratory program were evaluated to select the potential best mixtures for full-scale pavement slab evaluation. The desirable characteristics of concrete for pavement slabs, in terms of stress generation under loading, are high flexural strength, low MOE, and low CTE. Moreover, having low permeability and drying shrinkage is important for the long-term serviceability and durability of concrete pavement slabs.

All the hybrid ICC mixtures showed satisfied plastic and hardened properties for the rigid pavement applications. In particular, based on the *R*/*E* results from Fig. 3 (bottom right), the hybrid ICC mixtures show a great advantage for the potential fatigue resistance, which will be evaluated by both full-scale tests and numerical analysis. Thus, the hybrid ICC mixtures, such as ICC-SRA, ICC-PMF, and ICC-OAG 100, were selected to be evaluated in the full-scale field program. The test slab designation and their corresponding concrete mixtures are shown in Table 5.

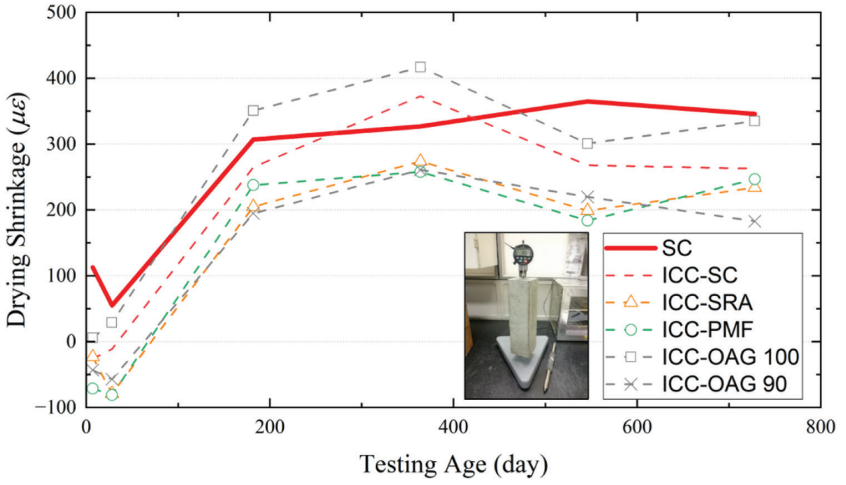


*Fig. 4—Drying shrinkage of ICC mixtures for 2 years.*

**Table 5—Slab designation and corresponding selected concrete mixtures for evaluation**

| Selected concrete mixtures | SC without ICC | ICC-SRA | ICC-PMF | ICC-OAG 100 |
|---|---|---|---|---|
| Cement, kg/m$^3$ | 256.3 | 256.3 | 256.3 | 256.3 |
| Fly ash, kg/m$^3$ | 64.1 | 64.1 | 64.1 | 64.1 |
| Water, kg/m$^3$ | 141.0 | 141.0 | 141.0 | 141.0 |
| Coarse aggregate 1, kg/m$^3$ | 894.7 | 1617.9 | 1006.2 | 936.8 |
| Coarse aggregate 2, kg/m$^3$ | 70.6 | — | — | 138.2 |
| Lightweight aggregate, kg/m$^3$ | — | 168.5 | 113.7 | 113.7 |
| Fine aggregate, kg/m$^3$ | 856.0 | 540.5 | 578.1 | 575.9 |
| Air entrainer, mL/kg | — | — | 1.3 | 0.2 |
| Water reducer, mL/kg | 2.9 | 2.9 | 3.3 | 2.9 |
| High-range water reducer, mL/kg | 4.9 | 2.7 | 3.3 | 2.5 |
| Shrinkage-reducing admixture, mL/kg | — | 2.9 | — | — |
| Synthetic microfiber, kg/m$^3$ | — | — | 0.9 | — |

## FULL-SCALE FIELD TEST PROGRAM

### Description of test slabs

This study aims to examine the feasibility of rigid pavement using hybrid ICC mixtures by considering long-term performance metrics. Given the challenges faced by prior research in predicting long-term structural performance, the present investigation employs an accelerated testing approach using an HVS. This study investigates the viable application of rigid pavement with the hybrid ICC mixtures in terms of short- and long-term performance. The full-scale test slabs were constructed to monitor the structural behavior subjected to HVS loading. Each test slab was 3.6 x 4.6 m (11.8 x 15.1 ft) in size and 23 cm (9 in.) in thickness, which represents a typical jointed plain concrete pavement (JPCP) slab. These test slabs were constructed over an existing 5 cm (2 in.) thick asphalt layer, which acted as a leveling course and provided the firm and consistent foundation for the concrete slabs, supported by a 27 cm (11 in.) limerock base layer. The full-scale test slabs were constructed, and HVS loading was applied after 130 days to evaluate the accelerated fatigue performance and the verification of the developed FE model. Only the two test slabs of SC and ICC-PMF were evaluated with the HVS due to the limited schedule of the HVS used.

The concrete mixtures used in the test slabs were evaluated for their fresh concrete properties at the time of the placement of the concrete slabs. At the same time, the samples were made to evaluate the properties of hardened concrete. Table 6 shows the tested plastic and hardened properties of the concrete mixtures compared with the corresponding standards. The workability rating was good for all the mixtures with respect to ease of placement and finishing. The air contents of all the concrete mixtures were within the allowable FDOT specification (1 to 6%). For the hardened concrete, all reported properties of the hybrid ICC mixtures were similar to those of the SC mixture. The strength results were as expected because earlier studies have reported that neither the use of ICC nor less than a 1% volume fraction of FRC helps improve the strength properties directly.[47,48]

### Instrumentation layout and installation

The test slabs were instrumented with fiber-optic sensors (FOS) to measure dynamic strains in the slabs. The embedded FOS gauges were placed at the mid-edge of the slab on the HVS wheel's path. For each gauge location, two FOS gauges were placed at a depth of 5 cm (2 in.) from the concrete surface and 5 cm from the bottom of the concrete layer in the longitudinal direction. Figure 5 presents the instrumentation layout for the test slabs with the loading locations of the falling weight deflectometer (FWD) and HVS. HVS loading was applied using a single wide tire with a contact pressure of 827 kPa (120 psi) and a load of 53 kN

**Table 6—Plastic and hardened properties of concrete used in test slabs**

| Selected concrete mixtures | SC without ICC | ICC-SRA | ICC-PMF | ICC-OAG 100 |
|---|---|---|---|---|
| Slump, cm | 7.0 | 7.0 | 8.9 | 16.5 |
| Air content, % | 4.4% | 2.7% | 5.1% | 1.3% |
| Unit weight, kg/m$^3$ | 2226.6 | 2210.6 | 2114.4 | 2210.6 |
| Compressive strength, MPa | 37.3 | 38.5 | 29.1 | 35.9 |
| Modulus of elasticity, MPa | 29,647 | 27,924 | 25,855 | 26,545 |
| Modulus of rupture, kPa | 5688 | 5792 | 4929 | 5206 |

Note: 1 MPa = 145 psi; 1 kPa = 0.145 psi.

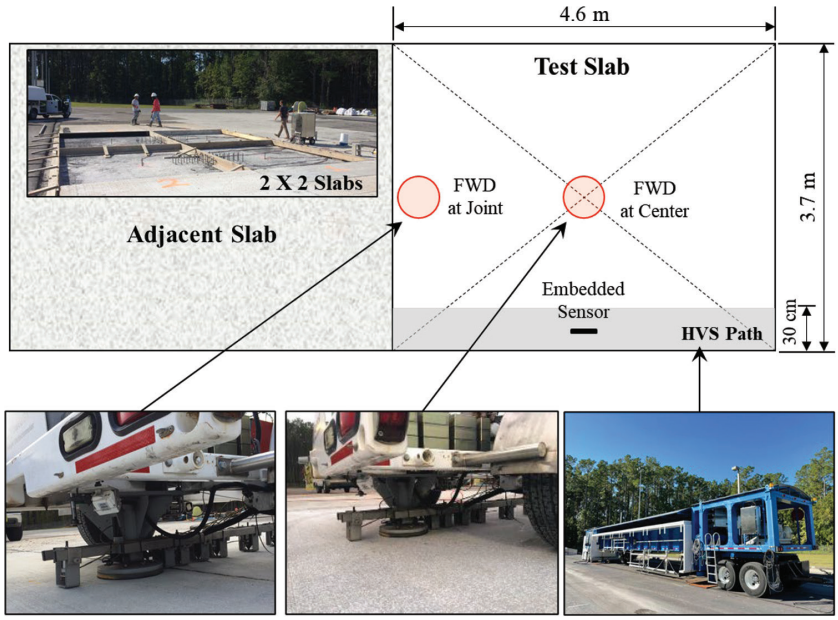


*Fig. 5—Instrumentation design for FWD and HVS testing.*

(12 kip), traveling at approximately 12 km/h (7 mph) in a single direction. During HVS testing, dynamic strain data from the tested slab were recorded at every 1-hour interval for 200 seconds to capture the dynamic strains caused by 20 HVS wheel passes.

## NUMERICAL EVALUATION OF CRITICAL STRESS ANALYSIS

### Validation of FE model

Figure 6 shows the three-dimensional (3-D) FE model developed for the critical stress analysis of the test slabs. The effects of temperature differential in the concrete slab were considered in the critical stress analysis. The concrete is characterized by its elastic modulus, Poisson's ratio, and CTE. The properties of the concrete used in the model were initially obtained from the measured properties of the sampled concrete. The effective elastic modulus of the subgrade and load transfer across the joint were obtained through the back-calculation method by matching the analytical to the measured FWD deflections.[49] Surface deflections in the concrete pavement caused by a 53 kN (12 kip) FWD were used to estimate the values of the effective elastic modulus of the subgrade and the stiffness of the springs for the load transfer at the joints. Figure 7 shows one of the examples of the matched deflection basins from the back-calculation process for estimating joint spring stiffness.

### Verification of FE model

Using the filtered strain data, the behavior of longitudinal tensile strains caused by a 53 kN (12 kip) HVS load was determined. To compare the measured strains with the computed strains, a similar condition of temperature differential in the concrete slab was considered. The maximum measured strains obtained under the condition of a close-to-zero temperature differential in the concrete slabs were used for this purpose. The selected measured strain data were obtained from the following testing times: 1) Trial 16 at 12:30 pm for SC; and 2) Trial 21 at 8:48 am for ICC-PMF, when the measured temperature differential was nearly zero. The measured maximum strains from the strain gauges in the test slabs compared to the computed strain are shown in Fig. 8, which shows good matching between the measured and computed values.

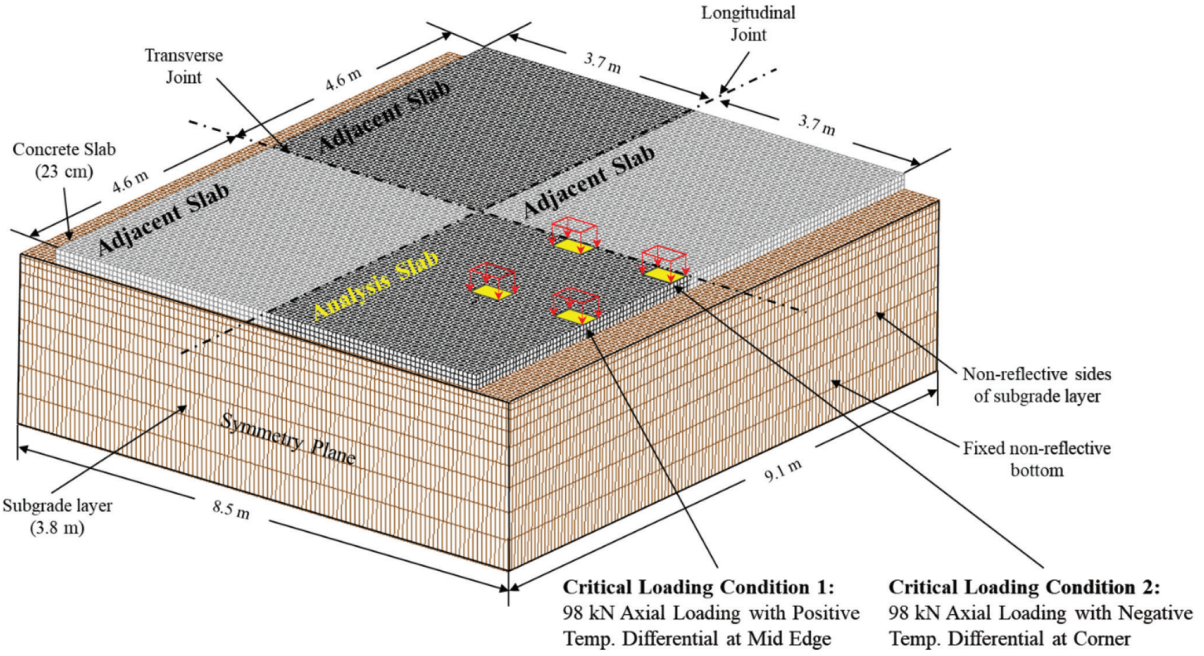


*Fig. 6—3-D FE model for four test slabs and location of critical loading conditions with combined environmental and wheel loading.*

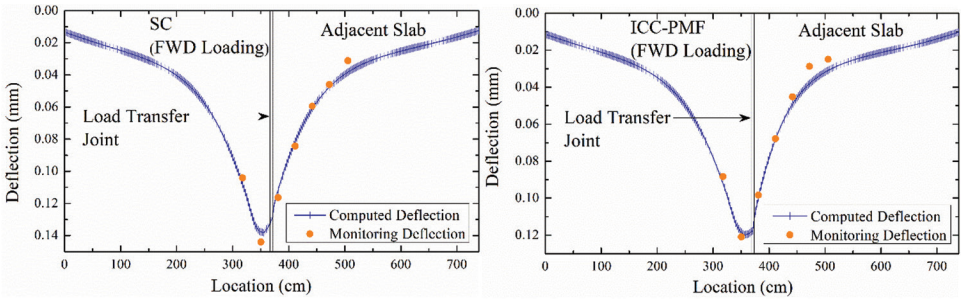


*Fig. 7—Determination of spring stiffness across joint using FWD basin: (left) comparison between calculated deflection and recorded deflection by loading on SC mixture; and (right) ICC-PMF.*

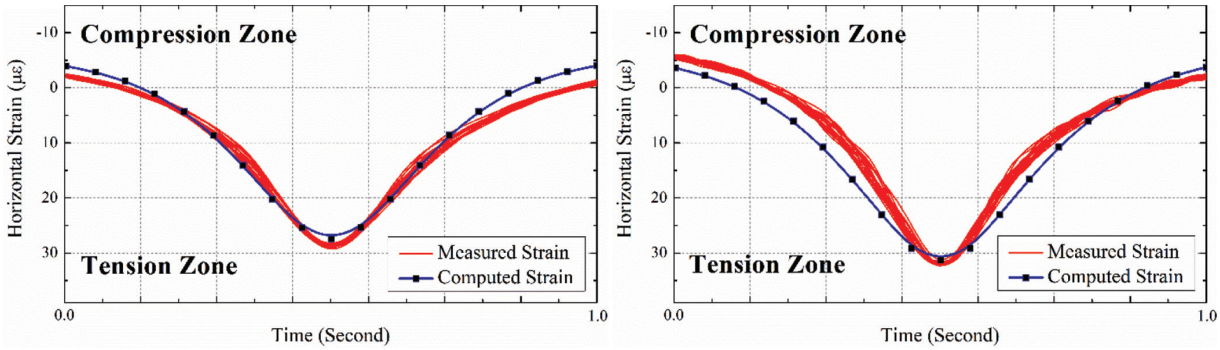


*Fig. 8—Comparison between measured strain from sensor under HVS loading 20 times and computed strain of: (left) SC mixture; and (right) ICC-PMF.*

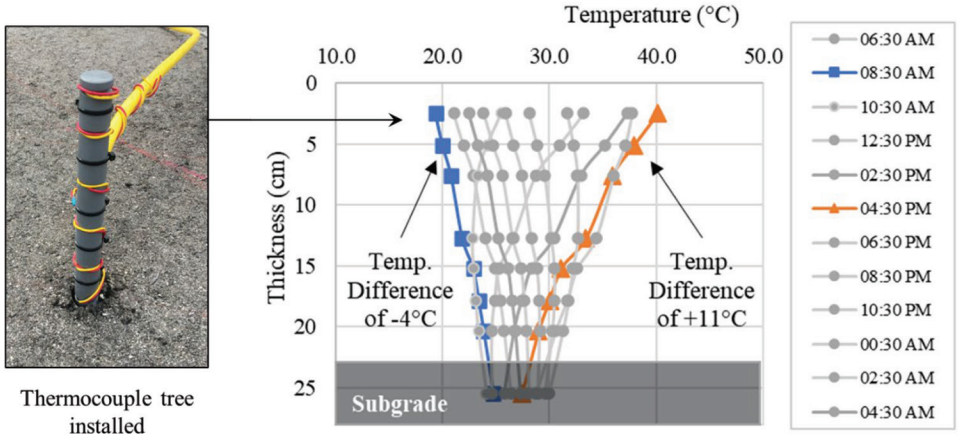


*Fig. 9—Recorded temperature differential to validate inputted environmental loading for critical stress analysis.*

**Table 7—Computed maximum stresses and stress-to-strength ratios for test slabs**

| Selected concrete mixtures | Temperature differential, °C | MOE, MPa | MOR, kPa | Computed stress, kPa | | Stress-to-strength ratio | |
|---|---|---|---|---|---|---|---|
| | | | | Corner | Mid-edge | Corner | Mid-edge |
| SC | +11.1 | 29,647 | 5688 | 1896 | 3495 | 0.33 | **0.61** |
| | –5.5 | 29,647 | 5688 | 1290 | 1080 | 0.23 | 0.19 |
| ICC-SRA | +11.1 | 27,923 | 5792 | 1695 | 3102 | 0.29 | **0.54** |
| | –5.5 | 27,923 | 5792 | 1156 | 934 | 0.20 | 0.16 |
| ICC-PMF | +11.1 | 25,855 | 4929 | 2143 | 2612 | 0.43 | **0.53** |
| | –5.5 | 25,855 | 4929 | 1153 | 1142 | 0.23 | 0.23 |
| ICC-OAG 100 | +11.1 | 26,544 | 5205 | 1537 | 2865 | 0.30 | **0.55** |
| | –5.5 | 26,544 | 5205 | 1076 | 852 | 0.21 | 0.16 |

Note: Maximum numbers within each concrete mixture are marked in bold.

## Assessment of critical stress analysis

A main design requirement for a rigid pavement should be the prevention of fatigue failure. All mechanistic-based designs use linear-elastic stress analysis to predict the stress-to-strength ratio as the indicator of fatigue resistance.[50,51] To compare the fatigue resistance of the test slabs, the validated FE model was used to calculate the maximum tensile stress under a critical load-temperature condition. Table 7 summarizes the results of the critical stress analysis, which show that the maximum stresses and maximum stress-to-strength ratios were obtained when a 98 kN (22 kip) axle load was applied to the mid-edge of the pavement slab with a temperature differential of +11.1°C (52°F). Furthermore, the slab's temperature was recorded for 4 months from the thermocouple trees along the slab depth, as shown in Fig. 9, and this revealed that the designed temperature differential used in the critical stress analysis was acceptable.

The computed stress-to-strength ratios for SC, ICC-SRA, ICC-PMF, and ICC-OAG 100 were 0.61, 0.54, 0.53, and 0.55, respectively, when applied to the critical loading condition proven by Tia et al.[44] and field monitoring. Because fatigue models commonly take advantage of a stress-to-strength ratio to predefine the slab's performance of fatigue cracking,[43] this result indicates that the hybrid ICC

mixtures outperformed the SC mixture in terms of fatigue cracking resistance, as evidenced by the lower stress-to-strength ratios. In line with critical stress analysis to predict fatigue resistance, an accelerated pavement test using HVS was conducted. The test slabs of SC and ICC-PMF, which had low computed stress-to-strength ratios (0.61 and 0.53, respectively), did not show any visible cracks after HVS loading. Figure 10 shows the pictures of the surfaces of all slabs after HVS loading.

## LIFE-CYCLE COST ANALYSIS ON USE OF ICC IN PAVEMENT APPLICATIONS

### Predicted service life based on AASHTO

This study undertakes a life-cycle cost analysis (LCCA) to examine the application of ICC with OAG, SRA, and PMFs in concrete pavement, compared with SC (as the control condition). The AASHTO design equation for concrete pavement[52] was employed to scrutinize the potential performance of the Class I (pavement) concrete mixtures, as shown in Eq. (3).

$$\log_{10}W_{18} = Z_R \cdot S_o + 7.35\log_{10}(D+1) - 0.06 + \frac{\log_{10}\left(\frac{\Delta PSI}{3}\right)}{1+\left(\frac{1.64\times10^7}{(D+1)^{8.46}}\right)} + (4.22 - 0.32p_t) \times \log_{10}\frac{S_c' \cdot C_d(D^{0.785}-1.132)}{215.63J\left(\frac{D^{0.75}-18.42}{\left(\frac{E_c}{k}\right)^{0.25}}\right)} \quad (3)$$

This design equation originated from the AASHTO Road Test, conducted in Ottawa, IL, in 1993. It establishes a correlation between the number of 80 kN (18 kip) equivalent single-axle loads (ESALs) that a pavement can carry before reaching a predetermined terminal serviceability index as a function of various relevant pavement design parameters. A conventional rigid pavement in Florida, featuring a slab thickness of 23 cm (9 in.), serves as the model for this hypothetical analysis.

The subsequent values were employed for the various design parameters: where $W_{18}$ represents the predicted number of 80 kN (18 kip) ESALs, $Z_R$ is the standard normal deviate, with a value of 0.35; $S_0$ denotes the combined standard error of the traffic prediction and performance prediction, which is assigned a value of –1.645; $D$ is the pavement slab thickness of 23 cm (9 in.); $\Delta PSI$ indicates the disparity between the initial design serviceability index ($p_o$) and the design terminal serviceability index ($p_t$), with $p_t$ being 1.9; $S_c'$ denotes the concrete flexural strength; $J$ is the load transfer coefficient used to adjust for load transfer characteristics of a specific design valued at 3.2; $C_d$ is the drainage coefficient and is set at 1; $E_c$ indicates the concrete modulus of elasticity; and $k$ represents the modulus of subgrade reaction, established at 2.76 MPa (400 psi).[14,53] Using an annual average daily traffic (AADT) metric of 48,500 for Archer Road, Gainesville, FL, from the FDOT database[54] (equivalent to an annual $W_{18}$ of 408,800), Table 8 presents the estimated pavement service lives for the concrete mixtures studied. All ICC mixtures are projected to have a longer service life than SC based on the analysis of service life predictions. These outcomes can be attributed to the hybrid ICC mixtures possessing a higher flexural strength and lower MOE than the SC mixture.

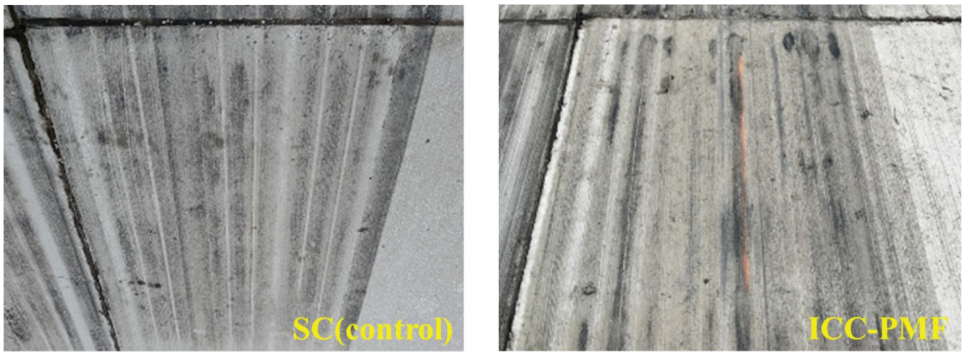


*Fig. 10—Test slabs surface after HVS loading: (left) no crack on surface of SC mixture; and (right) no crack on surface of ICC-PMF.*

**Table 8—Calculated $W_{18}$ using AASHTO design and associated estimated service life**

| Ten concrete mixtures | $S_c'$, MPa | $E$, MPa | Total calculated $W_{18}$ | Service life of pavement | |
|---|---|---|---|---|---|
| | | | | Year | Mixture/SC |
| SC (control) | 5.08 | 34,335 | 7,391,536 | 18.1 | 1.00 |
| ICC-SRA | 5.47 | 32,405 | 9,735,108 | 23.8 | 1.31 |
| ICC-PMF | 5.37 | 33,232 | 9,019,921 | 22.1 | 1.22 |
| ICC-OAG 100 | 5.67 | 33,508 | 10,845,391 | 26.5 | 1.46 |

**Table 9—Concrete cost for one lane mile of rigid pavement**

| Ten concrete mixtures | Service life of pavement, years | Cost per $yd^3$, $ | Total concrete cost, $ | EAC at 0%, $ | EAC at 5%, $ |
|---|---|---|---|---|---|
| SC (control) | 18.1 | 157.9 | 277,981 | 15,358 (4) | 23,698 (4) |
| ICC-SRA | 23.8 | 181.8 | 320,051 | 13,448 (3) | 23,297 (3) |
| ICC-PMF | 22.1 | 159.2 | 280,149 | 12,677 (2) | 21,229 (2) |
| ICC-OAG 100 | 26.5 | 154.8 | 272,473 | 10,282 (1) | 18,777 (1) |

Note: 1 $yd^3$ = 0.765 $m^3$; $ is USD.

### Life-cycle cost analysis

In this study, only the material costs were incorporated into the LCCA for the rigid pavement. Unit costs for each concrete mixture were computed by aggregating the material expenses for all constituents within each mixture. To illuminate the genuine expenditure related to rigid pavement, the comprehensive material cost for a concrete lane mile, assuming a thickness of 23 cm (9 in.) and a width of 3.65 m (12 ft), was calculated for each concrete mixture, the details of which are elucidated in Table 9. Using the predicted service life of each concrete, as presented in Table 8, in conjunction with the unit cost, the equivalent annual cost (EAC) was computed for each concrete mixture by applying Eq. (4).

$$\text{Equivalent annual cost (EAC)} = \frac{PW \times i}{\frac{[(1+i)^n - 1]}{(1+i)^n}} \quad (4)$$

where $i$ represents the interest rate per year; $PW$ signifies the present worth total cost; and $n$ stands for the years of service life. Table 9 presents the EAC computations using interest rates of 0 and 5%. In scenarios that preclude interest, all hybrid concrete mixtures exhibit a lower EAC than SC. Employing an interest rate of 5%, the same hybrid concrete mixtures demonstrated a reduced EAC relative to SC. Notably, the concrete mixtures yielding the lowest EAC were the concretes incorporating both ICC and OAG (ICC-OAG 100). Their relative EACs were 67% and 79%, compared with SC, when analyzed with interest rates of 0% and 5%, respectively. These findings suggest that the hybrid ICC is a potentially promising concrete design for pavements when considering aspects of extended service life and cost-effectiveness.

## CONCLUSIONS AND RECOMMENDATIONS

This paper presents comprehensive results that describe the behavior of internally cured concrete (ICC) mixtures with three possible enhanced techniques incorporating shrinkage-reducing admixture (SRA), polymeric microfibers (PMFs), and optimized aggregate gradation (OAG). To evaluate the ICC mixtures for rigid pavement applications, a laboratory testing program, full-scale field-testing program, critical stress analysis, and life-cycle cost analysis (LCCA) were conducted to evaluate the potential benefits of hybrid ICC mixtures. A summary of the conclusions from the results presented in this paper is as follows:

- All concrete mixtures, with or without incorporating internal curing (IC), exhibited satisfactory plastic, hardened, and durability properties suitable for pavement applications.
- Each ICC mixture incorporating SRA, PMFs, and OAG exhibited favorable results of the increased modulus of rupture (MOR)-modulus of elasticity (MOE) ratio ($R/E$) when compared with the non-ICC concrete mixture.
- The OAG design method is also effective in ICC mixtures because the concrete strength did not decrease when the cement content was reduced by 10%.
- From the validated finite element (FE) analysis, the ICC-PMF slab had a lower stress-to-MOR ratio than the standard concrete (SC) slab, indicating potentially better performance. This is due to the ICC's enhanced properties of lower MOE, lower coefficient of thermal expansion (CTE), lower density, and increased toughness when compared with ordinary non-ICC concrete (SC).
- Based on the LCCA, the hybrid ICC is a promising concrete design for rigid pavements due to its extended service life and cost-effectiveness.
- From the overall analysis, all hybrid ICC mixtures are shown to be suitable for use in rigid pavements and have better-than-expected performances than SC.

This study conducted a comprehensive research program encompassing laboratory tests, numerical analysis, field evaluation, and LCCA to assess the potential of hybrid ICC mixtures for rigid pavements. Given the limitations within these scopes, the authors recommend the following considerations for future studies:

- This paper assessed the feasibility of hybrid ICC mixtures using SRA, PMFs, and OAG. A deeper investigation into the intricate mechanisms influencing the properties of concrete for rigid pavements would likely provide valuable insights for future research.
- Surface friction is a crucial property for concrete mixtures in rigid pavements, warranting investigation with hybrid ICC mixtures.

## AUTHOR BIOS

**Sangyoung Han** *is an Assistant Professor in the Department of ICT Integrated Ocean Smart City Engineering at Dong-A University, Busan, South Korea. He received his PhD from The University of Texas at Austin, Austin, TX, in 2022. His research interests include the concrete mixture characteristics and analysis of reinforced and prestressed concrete structures.*

**Thanachart Subgranon** *is a Professional Engineer at Fugro, responsible for deep foundation testing. He specializes in bidirectional testing. He received his PhD in civil engineering at the University of Florida, Gainesville, FL, in 2020. His research interests include concrete pavements and materials, accelerated pavement testing, and instrumentation for pavements and materials research.*

**Hung-Wen Chung** *is the Field Services Manager for the Gainesville satellite office of ECS Florida, LLC. He received his PhD from the University of*

*Florida in 2020. He has over 10 years of experience specializing in concrete and construction materials, with a focus on pavement and structures.*

**Kukjoo Kim** *is a Professional Engineer at the Defense Installations Agency, Ministry of National Defense, South Korea. He received his PhD from the University of Florida in 2017. His research interests include ultra-high-performance concrete and analysis of protective structures against blast loadings.*

**Mang Tia** *is a Professor of civil engineering at the University of Florida, where he has been a faculty member since 1982. His research interests include concrete pavements and materials, asphalt pavements and materials, accelerated pavement testing, and instrumentation for pavements and materials research.*

## ACKNOWLEDGMENTS

This work was supported by the Dong-A University research fund.

## REFERENCES

1. Russell, H. G.; Miller, R. A.; Ozyildirim, H. C.; and Tadros, M. K., "Compilation and Evaluation of Results from High-Performance Concrete Bridge Projects, Volume I: Final Report," *Report* No. FHWA HRT-05-056, Federal Highway Administration, McLean, VA, 2006, 180 pp.

2. Castro, J.; Spragg, R.; and Weiss, J., "Water Absorption and Electrical Conductivity for Internally Cured Mortars with a W/C between 0.30 and 0.45," *Journal of Materials in Civil Engineering*, ASCE, V. 24, No. 2, Feb. 2012, pp. 223-231.

3. Shattaf, N. R.; Alshamsi, A. M.; and Swamy, R. N., "Curing/Environment Effect on Pore Structure of Blended Cement Concrete," *Journal of Materials in Civil Engineering*, ASCE, V. 13, No. 5, Oct. 2001, pp. 380-388. doi: 10.1061/(ASCE)0899-1561(2001)13:5(380)

4. Bentz, D. P., "Influence of Curing Conditions on Water Loss and Hydration in Cement Pastes with and without Fly Ash Substitution," NISTIR *Report* No. 6886, National Institute of Standards and Technology, Gaithersburg, MD, 2002, 21 pp.

5. Sant, G.; Lura, P.; and Weiss, J., "Measurement of Volume Change in Cementitious Materials at Early Ages: Review of Testing Protocols and Interpretation of Results," *Transportation Research Record: Journal of the Transportation Research Board*, V. 1979, No. 1, Jan. 2006, pp. 21-29. doi: 10.1177/0361198106197900104

6. RILEM Technical Committee 196-ICC, "Internal Curing of Concrete: State-of-the-Art Report," K. Kovler and O. M. Jensen, eds., RILEM Publications SARL, Bagneux, France, 2007, 141 pp.

7. ACI Committee 231, "Report on Early-Age Cracking: Causes, Measurement, and Mitigation (ACI 231R-10) (Reapproved 2020)," American Concrete Institute, Farmington Hills, MI, 2010, 46 pp.

8. Weiss, J., "Internal Curing for Concrete Pavements," Tech Brief No. FHWA-HIF-16-006, Federal Highway Administration, Washington, DC, 2016, 7 pp.

9. Jensen, O. M., and Hansen, P. F., "Autogenous Deformation and RH-Change in Perspective," *Cement and Concrete Research*, V. 31, No. 12, Dec. 2001, pp. 1859-1865. doi: 10.1016/S0008-8846(01)00501-4

10. Cusson, D., and Hoogeveen, T., "Internal Curing of High-Performance Concrete with Pre-soaked Fine Lightweight Aggregate for Prevention of Autogenous Shrinkage Cracking," *Cement and Concrete Research*, V. 38, No. 6, June 2008, pp. 757-765. doi: 10.1016/j.cemconres.2008.02.001

11. Radlinska, A.; Rajabipour, F.; Bucher, B.; Henkensiefken, R.; Sant, G.; and Weiss, J., "Shrinkage Mitigation Strategies in Cementitious Systems: A Closer Look at Differences in Sealed and Unsealed Behavior," *Transportation Research Record: Journal of the Transportation Research Board*, V. 2070, No. 1, Jan. 2008, pp. 59-67. doi: 10.3141/2070-08

12. Lopez, M.; Kahn, L. F.; and Kurtis, K. E., "Characterization of Elastic and Time-Dependent Deformations in High Performance Lightweight Concrete by Image Analysis," *Cement and Concrete Research*, V. 39, No. 7, July 2009, pp. 610-619. doi: 10.1016/j.cemconres.2009.03.015

13. Kim, H. K.; Jeon, J. H.; and Lee, H. K., "Workability, and Mechanical, Acoustic and Thermal Properties of Lightweight Aggregate Concrete with a High Volume of Entrained Air," *Construction and Building Materials*, V. 29, Apr. 2012, pp. 193-200. doi: 10.1016/j.conbuildmat.2011.08.067

14. Bentz, D. P., and Weiss, W. J., "Internal Curing: A 2010 State-of-the-Art Review," NISTIR *Report* No. 7765, National Institute of Standards and Technology, Gaithersburg, MD, 2011, 94 pp.

15. Byard, B. E.; Schindler, A. K.; Barnes, R. W.; and Rao, A., "Cracking Tendency of Bridge Deck Concrete," *Transportation Research Record: Journal of the Transportation Research Board*, V. 2164, No. 1, Jan. 2010, pp. 122-131. doi: 10.3141/2164-16

16. Jones, W. A., and Weiss, W. J., "Freezing and Thawing Behavior of Internally Cured Concrete," *Advances in Civil Engineering Materials*, V. 4, No. 1, 2015, pp. 144-155. doi: 10.1520/ACEM20140044

17. Wei, Y., and Hansen, W., "Characterization of Moisture Transport and Its Effect on Deformations in Jointed Plain Concrete Pavement," *Transportation Research Record: Journal of the Transportation Research Board*, V. 2240, No. 1, Jan. 2011, pp. 9-15. doi: 10.3141/2240-02

18. Amirkhanian, A. N., and Roesler, J. R., "Unrestrained Curling in Concrete with Fine Lightweight Aggregates," *Journal of Materials in Civil Engineering*, ASCE, V. 29, No. 9, Sept. 2017, p. 04017092. doi: 10.1061/(ASCE)MT.1943-5533.0001941

19. Johnson, A. M.; Smith, B. C.; Johnson, W. H.; and Gibson, L. W., "Evaluating the Effect of Slab Curling on IRI for South Carolina Concrete Pavements," *Report* No. FHWA-SC-10-04, South Carolina Department of Transportation, Columbia, SC, 2010, 30 pp.

20. Beckemeyer, C.; Khazanovich, L.; and Yu, H. T., "Determining Amount of Built-in Curling in Jointed Plain Concrete Pavement: Case Study of Pennsylvania 1-80," *Transportation Research Record: Journal of the Transportation Research Board*, V. 1809, No. 1, Jan. 2002, pp. 85-92. doi: 10.3141/1809-10

21. Lange, D. A., and Shin, H.-C., "Early Age Stresses and Debonding in Bonded Concrete Overlays," *Transportation Research Record: Journal of the Transportation Research Board*, V. 1778, No. 1, Jan. 2001, pp. 174-181.

22. Rao, C., and Darter, M. I., "Evaluation of Internally Cured Concrete for Paving Applications," Applied Research Associates, Inc., Champaign, IL, Sept. 2013, 121 pp.

23. Nmai, C. K.; Tomita, R.; Hondo, F.; and Buffenbarger, J., "Shrinkage-Reducing Admixtures," *Concrete International*, V. 20, No. 4, Apr. 1998, pp. 31-37.

24. Weiss, J., and Berke, N. S., "Admixtures for Reducing Shrinkage and Cracking," *Early Age Cracking in Cementitious Systems: Report of RILEM Technical Committee TC 181-EAS: Early Age Shrinkage Induced Stresses and Cracking in Cementitious Systems*, A. Bentur, ed., RILEM Publications SARL, Bagneux, France, 2002, pp. 323-336.

25. Gettu, R.; Roncero, J.; and Martin, M. A., "Study of the Behavior of Concrete with Shrinkage Reducing Admixtures Subjected to Long-Term Drying," *Concrete: Material Science to Application – A Tribute to Surendra P. Shah*, SP-206, P. Balaguru, A. Naaman, and W. Weiss, eds., American Concrete Institute, Farmington Hills, MI, 2002, pp. 157-166 pp.

26. Bentz, D. P.; Geiker, M. R.; and Hansen, K. K., "Shrinkage-Reducing Admixtures and Early-Age Desiccation in Cement Pastes and Mortars," *Cement and Concrete Research*, V. 31, No. 7, July 2001, pp. 1075-1085. doi: 10.1016/S0008-8846(01)00519-1

27. Weiss, J.; Lura, P.; Rajabipour, F.; and Sant, G., "Performance of Shrinkage-Reducing Admixtures at Different Humidities and at Early Ages," *ACI Materials Journal*, V. 105, No. 5, Sept.-Oct. 2008, pp. 478-486.

28. Lawler, J. S.; Zampini, D.; and Shah, S. P., "Microfiber and Macrofiber Hybrid Fiber-Reinforced Concrete," *Journal of Materials in Civil Engineering*, ASCE, V. 17, No. 5, Oct. 2005, pp. 595-604. doi: 10.1061/(ASCE)0899-1561(2005)17:5(595)

29. Passuello, A.; Moriconi, G.; and Shah, S. P., "Cracking Behavior of Concrete with Shrinkage Reducing Admixtures and PVA Fibers," *Cement and Concrete Composites*, V. 31, No. 10, Nov. 2009, pp. 699-704. doi: 10.1016/j.cemconcomp.2009.08.004

30. Plagué, T.; Desmettre, C.; and Charron, J.-P., "Influence of Fiber Type and Fiber Orientation on Cracking and Permeability of Reinforced Concrete under Tensile Loading," *Cement and Concrete Research*, V. 94, Apr. 2017, pp. 59-70. doi: 10.1016/j.cemconres.2017.01.004

31. Löfgren, I., "Fibre-Reinforced Concrete for Industrial Construction - A Fracture Mechanics Approach to Material Testing and Structural Analysis," PhD thesis, Chalmers University of Technology, Gothenburg, Sweden, 2005, 162 pp.

32. Roesler, J.; Bordelon, A.; Brand, A. S.; and Amirkhanian, A., "Fiber-Reinforced Concrete for Pavement Overlays: Technical Overview," InTrans Project *Report* No. 15-532, National Concrete Pavement Technology Center, Iowa State University, Ames, IA, Apr. 2019, 100 pp.

33. Biddle, D., "Fiber-Reinforced Concrete - Pavements," FORTA Corporation, Grove City, PA, Mar. 2020, 39 pp.

34. Lawler, J. S.; Wilhelm, T.; Zampini, D.; and Shah, S. P., "Fracture Processes of Hybrid Fiber-Reinforced Mortar," *Materials and Structures*, V. 36, No. 3, Apr. 2003, pp. 197-208.

35. Nobili, A.; Lanzoni, L.; and Tarantino, A. M., "Experimental Investigation and Monitoring of a Polypropylene-Based Fiber Reinforced Concrete Road Pavement," *Construction and Building Materials*, V. 47, Oct. 2013, pp. 888-895. doi: 10.1016/j.conbuildmat.2013.05.077

36. Mehta, P. K., and Monteiro, P. J. M., *Concrete: Microstructure, Properties, and Materials*, fourth edition, McGraw-Hill Education, New York, 2013.

37. Lindquist, W.; Darwin, D.; Browning, J.; McLeod, H. A. K.; Yuan, J.; and Reynolds, D., "Implementation of Concrete Aggregate Optimization," *Construction and Building Materials*, V. 74, Jan. 2015, pp. 49-56. doi: 10.1016/j.conbuildmat.2014.10.027

38. Kwan, A. K. H., and Ling, S. K., "Lowering Paste Volume of SCC through Aggregate Proportioning to Reduce Carbon Footprint," *Construction and Building Materials*, V. 93, Sept. 2015, pp. 584-594. doi: 10.1016/j.conbuildmat.2015.06.034

39. Cook, M. D.; Ley, M. T.; and Ghaeezadah, A., "Effects of Aggregate Concepts on the Workability of Slip-Formed Concrete," *Journal of Materials in Civil Engineering*, ASCE, V. 28, No. 10, Oct. 2016, p. 04016097. doi: 10.1061/(ASCE)MT.1943-5533.0001608

40. MDT, "Concrete Aggregate Combined Gradation Example," Montana Department of Transportation, Helena, MT, 2016, 6 pp.

41. FDOT, "Standard Specifications for Road and Bridge Construction: FY 2023-24," Florida Department of Transportation, Tallahassee, FL, 2023, 1299 pp.

42. AASHTO PP 84-17, "Standard Practice for Developing Performance Engineered Concrete Pavement Mixtures," American Association of State Highway and Transportation Officials, Washington, DC, 2017.

43. Smith, K. D., and Roesler, J. R., "Review of Fatigue Models for Concrete Airfield Pavement Design," *Airfield Pavements: Challenges and New Technologies: Proceedings of the 2003 Airfield Pavement Specialty Conference*, Las Vegas, NV, Sept. 2003, pp. 231-258.

44. Tia, M.; Wu, C. L.; Ruth, B. E.; Bloomquist, D.; and Choubane, B., "Field Evaluation of Rigid Pavements for the Development of a Rigid Pavement Design System—Phase IV," University of Florida, Gainesville, FL, 1989.

45. Wells, S. A.; Phillips, B. M.; and Vandenbossche, J. M., "Quantifying Built-in Construction Gradients and Early-Age Slab Deformation Caused by Environmental Loads in a Jointed Plain Concrete Pavement," *International Journal of Pavement Engineering*, V. 7, No. 4, 2006, pp. 275-289. doi: 10.1080/10298430600798929

46. Mehta, P. K., "Durability of Concrete—Fifty Years of Progress?" *Durability of Concrete: Second International Conference, Montreal, Canada 1991*, SP-126, V. M. Malhotra, ed., American Concrete Institute, Farmington Hills, MI, 1991, pp. 1-32.

47. Paul, Á., and Lopez, M., "Assessing Lightweight Aggregate Efficiency for Maximizing Internal Curing Performance," *ACI Materials Journal*, V. 108, No. 4, July-Aug. 2011, pp. 385-393.

48. ACI Committee 544, "Report on Fiber Reinforced Concrete (ACI 544.1R-96) (Reapproved 2009)," American Concrete Institute, Farmington Hills, MI, 1996, 66 pp.

49. Von Quintus, H. L., and Simpson, A. L., "Back-Calculation of Layer Parameters for LTPP Test Sections, Volume II: Layered Elastic Analysis for Flexible and Rigid Pavements," *Report* No. FHWA-RD-01-113, Federal Highway Administration, McLean, VA, 2002, 146 pp.

50. Darter, M.; Khazanovich, L.; Snyder, M.; Rao, S.; and Hallin, J., "Development and Calibration of a Mechanistic Design Procedure for Jointed Plain Concrete Pavements," *Proceedings of the 7th International Conference on Concrete Pavements: The Use of Concrete in Developing Long-Lasting Pavement Solutions for the 21st Century*, Orlando, FL, Sept. 2001, pp. 113-131.

51. Packard, R. G., and Tayabji, S. D., "New PCA Thickness Design Procedure for Concrete Highway and Street Pavements," *Proceedings of the Third International Conference on Concrete Pavement Design and Rehabilitation*, Purdue University, West Lafayette, IN, Apr. 1985, pp. 225-236.

52. AASHTO, "AASHTO Guide for Design of Pavement Structures 1993," American Association of State Highway and Transportation Officials, Washington, DC, 1993, 624 pp.

53. Mindess, S.; Young, J. F.; and Darwin, D., *Concrete*, second edition, Prentice Hall PTR, Hoboken, NJ, 2002, 644 pp.

54. FDOT, "Florida Department of Transportation Traffic Information," Florida Department of Transportation, Tallahassee, FL, https://www.fdot.gov/statistics/trafficdata/default.shtm. (last accessed Apr. 4, 2024)